*Thermochimica Acta*, 236 (1994) 239–248
Elsevier Science B.V., Amsterdam
*SSDI* 0040-6031(93)01601-X

# Heat transfer inside emulsions. Determination of the DSC thermograms.
## Part 2. Melting of the crystallized droplets

J.P. Dumas *, Y. Zeraouli and M. Strub

*Laboratoire de Thermodynamique et Energétique, Université de Pau et des Pays de l'Adour, Avenue de l'Université, 64000 Pau, France*

(Received 3 May 1993; accepted 12 September 1993)

### Abstract

A model is presented to explain the shape of the thermogram obtained by differential scanning calorimetry of the melting of the crystallized droplets of an emulsion. This model is entirely different from the model presented in Part 1 of this study concerning the crystallization of undercooled liquid droplets. In spite of the purity of the dispersed substance, significant temperature gradients are found, in contrast to the classical assumption of a uniform melting temperature. The model also gives the kinetics of the melting of the droplets which depends on their location.

LIST OF SYMBOLS

| | |
|---|---|
| $c$ | specific heat of the emulsion in $\mathrm{J\,K^{-1}\,kg^{-1}}$ |
| $h_{\mathrm{sl}}$ | specific latent heat of fusion ($>0$) in $\mathrm{J\,kg^{-1}}$ |
| $h$ | exchange coefficient for the droplet in $\mathrm{W\,m^{-2}\,s^{-1}}$ |
| $h^{\mathrm{ext}}$, $h'^{\mathrm{ext}}$ | external exchange coefficient for the cell in $\mathrm{W\,m^{-2}\,s^{-1}}$ |
| $k$ | heat conductivity of the emulsion in $\mathrm{W\,m^{-1}\,K^{-1}}$ |
| $n_{\mathrm{t}}$ | total number of droplets per unit volume in $\mathrm{m^{-3}}$ |
| $P$ | mass fraction of the dispersed substance |
| $\dot{q}$ | heat source in $\mathrm{J\,m^{-3}\,s^{-1}}$ |
| $R_0$ | inner radius of the cylinder in m |
| $t$ | time |
| $T(r, z, t)$ | temperature at $r$, $z$ and $t$ in °C |
| $T_{\mathrm{F}}$ | melting temperature in °C |
| $T_{\infty}(t)$ | programmed temperature of the bath in °C |
| $T_0$ | initial temperature in °C |
| $X(r, z, t)$ | proportion of the droplet which is melted |
| $\nabla$ | gradient or divergence operator |

---

* Corresponding author.

*Greek letters*

| | |
|---|---|
| $\alpha$ | diffusivity of the emulsion in $m^2\,s^{-1}$ |
| $\beta$ | heating rate ($>0$) in $°C\,h^{-1}$ |
| $\rho$ | mass density of the emulsion in $kg\,m^{-3}$ |

## INTRODUCTION

In Part 1 of this work [1], we proposed a model describing the heat transfers during the crystallization of undercooled droplets of an emulsion in the small cell of a differential scanning calorimeter. This model described with accuracy the shape of the thermograms. It was also concluded that the classical assumption in differential scanning calorimetry (DSC), i.e. the uniformity of the temperature inside the cell [2, 3], is not adequate to describe the DSC thermogram.

This is also the case, upon heating, for melting of the crystallized droplets. For the melting of a pure substance, the classical assumption of the uniformity of the temperature in the cell gives the theoretical DSC thermogram in Fig. 1 [2, 3]. The straight line at the beginning of the peak corresponds to the strictly constant melting temperature $T_F$; the end of the peak has an exponential shape, characteristic of the return to equilibrium. But the experimental thermogram in Fig. 2 is significantly different. It detects a beginning of melting before the melting temperature $T_F$. This could mainly be explained by the impurity of the dispersed substance, the surfactant that was chosen being soluble only in the emulsifying medium. We will not take into account this distortion, assuming in the model the perfect purity of the substance. Moreover, the top of the peak is rounded and its tail is quite different. For a long time it was suspected that this difference is due to heat transfers inside the cell. Therefore, the experimental estimation of these heat transfers by the "factors of form" was applied with success to determine the temperatures of the transformations. However no information is given on the detail of these transfers [4].

In this Part 2, we represent another description for the melting of the droplets of an emulsion. It is based on a model that takes into account the heat transfers applied to the small cell used in DSC [5].

## MODEL FOR THE MELTING OF THE DROPLETS OF AN EMULSION

As in the case of the crystallization, the model is based on the heat conduction equation. The difference is that the heat source $\dot{q}$ is endothermic, i.e. a heat sink

$$\frac{\partial T}{\partial t} = \alpha \nabla^2 T + \frac{\dot{q}}{\rho c} \qquad (1)$$

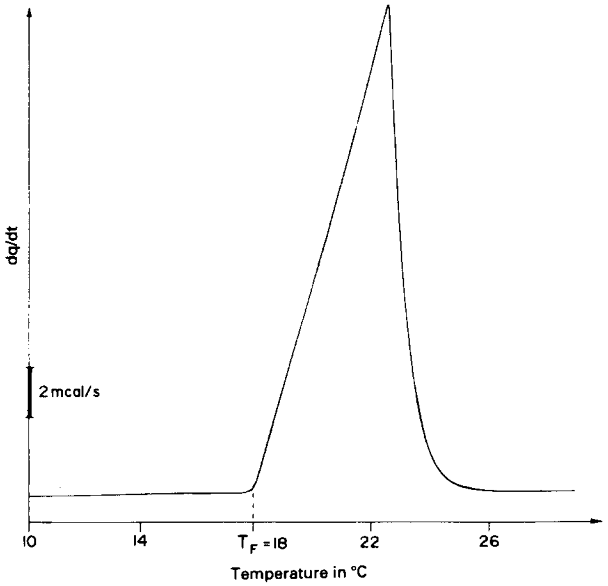

Fig. 1. Example of a thermogram predicted for the melting of a pure substance, under the uniform temperature assumption.

where $\alpha$ is the diffusivity of the emulsion, $\rho$ its density, $c$ its specific heat and where the sink $\dot{q}$ is given per unit time and unit volume.

Each droplet is a sink of energy because there is a difference between $T_g$, the temperature of the inner part of the droplet, and $T$, the temperature of the emulsifying medium which surrounds it. This difference can be explained by the fact that each droplet is actually surrounded by a relatively thick layer of surfactant molecules.

Except at the time of melting, the energy balance for each droplet is (Fig. 3)

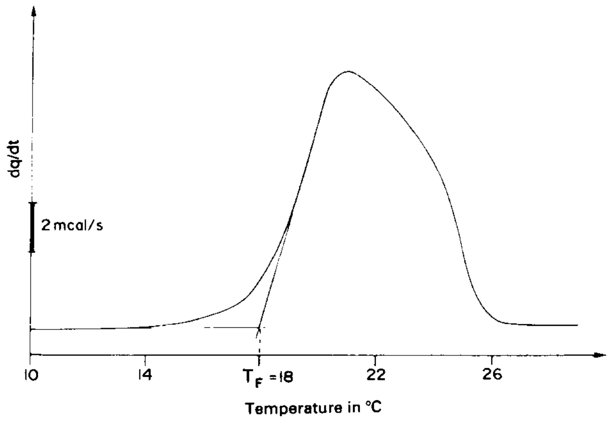

Fig. 2. Example of an experimental thermogram.

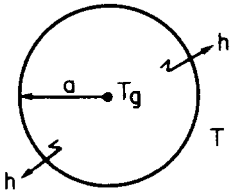

Fig. 3. Scheme of the droplet when not melting.

$$\rho_0 V C_0 \frac{\mathrm{d}T_g}{\mathrm{d}t} = -h(T_g - T)S \tag{2}$$

where $V$ is the volume of the droplet, $S$ its area, $\rho_0$ the density of the droplet and $c_0$ its specific heat; $h$ is an exchange coefficient characteristic of the thermal resistance due to the layer of surfactant.

During the melting (Fig. 4), the energy balance is quite different because $T_g = T_F$ and the exchanged heat proceeds from the fraction of crystal which is melting

$$\rho_0 V h_{sl} \frac{\mathrm{d}X}{\mathrm{d}t} = -h(T_F - T)S \tag{3}$$

where $h_{sl}$ is the latent heat of fusion and $X$ the proportion of droplet already melted.

The droplet temperature remains constant at $T_F$ as long as $0 < X < 1$, until the melting of the last part of the crystal ($X = 1$).

Thus, for the unit volume, the energy sink is

$$\dot{q} = -h(T_g - T)Sn_t$$

where $n_t = \rho P/\rho_0 V$ is the total number of droplets per unit emulsion volume. $P$ is the mass fraction of the emulsion defined as the ratio between the mass of the dispersed liquid and the mass of the emulsion.

Finally, we have

$$\dot{q} = \frac{-3\rho P h}{a\rho_0}(T - T_g) \tag{4}$$

where $a$ is the mean radius of the droplets; $(T - T_g)$ is given either by eqn. (2) if $X = 0$ or $X = 1$, or by eqn. (3) ($T_g = T_F$) if $0 < X < 1$.

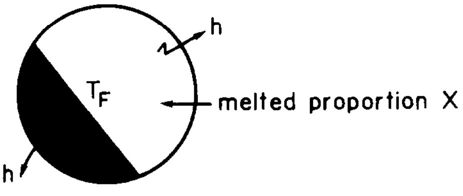

Fig. 4. Scheme of the droplet during melting.

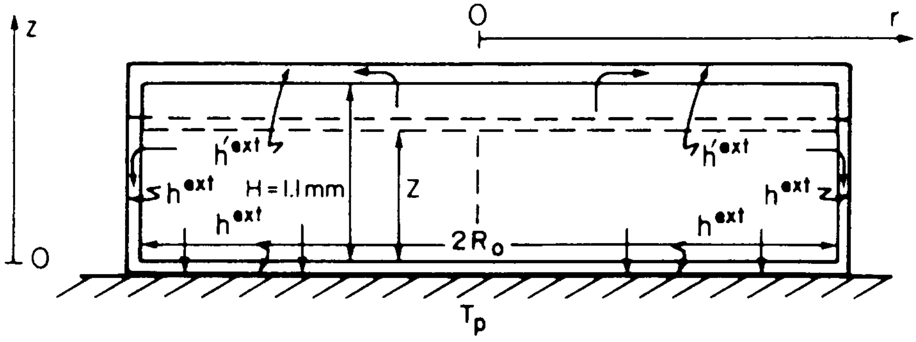

Fig. 5. Scheme of the cell.

## STUDY OF THE DSC THERMOGRAMS

The principle of differential scanning calorimetry was outlined in Part 1 [1]. The apparatus (Perkin-Elmer DSC4) gives $\mathrm{d}q/\mathrm{d}t$, the difference between the heat powers maintaining the plate supporting the active cell containing the emulsion and the plate supporting the reference cell

$$\frac{\mathrm{d}q}{\mathrm{d}t}=\left(\frac{\mathrm{d}q}{\mathrm{d}t}\right)_{\text{active cell}}-\left(\frac{\mathrm{d}q}{\mathrm{d}t}\right)_{\text{reference}}$$

As indicated in Part 1 [1], the power exchanged at the reference plate is practically constant and equal to $(\mathrm{d}q/\mathrm{d}t)_{\mathrm{ref}}=\beta c_{\mathrm{R}}$, $\beta$ being the heating rate. So, to simplify the model we will omit this term from the calculation of $\mathrm{d}q/\mathrm{d}t$ (equivalent to a shift in the baseline).

We have modelled the active cell with a cylinder whose dimensions are $2R_0=4.25$ mm for the diameter and $Z=0.82$ mm for the height of the emulsion (Fig. 5). $T$, $T_{\mathrm{g}}$ and $X$ depend on the two space variables $r$ and $z$ and on the time $t$. The systems to be solved are:

(i) Before, $T_{\mathrm{g}}<T_{\mathrm{F}}$ $(X=0)$, or after, $T_{\mathrm{g}}>T_{\mathrm{F}}$ $(X=1)$, the melting

$$\frac{\partial T}{\partial t}=\alpha\left(\frac{\partial^2 T}{\partial r^2}+\frac{1}{r}\frac{\partial T}{\partial r}+\frac{\partial^2 T}{\partial z^2}\right)-\frac{3hP}{\rho_0 ca}(T-T_{\mathrm{g}}) \tag{5}$$

$$\frac{\mathrm{d}T_{\mathrm{g}}}{\mathrm{d}t}=\frac{3h}{\rho_0 c_0 a}(T-T_{\mathrm{g}}) \tag{6}$$

(ii) During the melting: $T\geqslant T_{\mathrm{F}}$ and $0<X<1$ $(T_{\mathrm{g}}=T_{\mathrm{F}})$

$$\frac{\partial T}{\partial t}=\alpha\left(\frac{\partial^2 T}{\partial r^2}+\frac{1}{r}\frac{\partial T}{\partial r}+\frac{\partial^2 T}{\partial z^2}\right)-\frac{3hP}{\rho_0 ca}(T-T_{\mathrm{F}}) \tag{7}$$

$$\frac{\mathrm{d}X}{\mathrm{d}t}=\frac{3h}{\rho_0 h_{\mathrm{sl}} a}(T-T_{\mathrm{F}}) \tag{8}$$

To take into account the air between the emulsion and the cover of the cell, we consider two different heat exchange coefficients $h^{\mathrm{ext}}$ and $h'^{\mathrm{ext}}$ (Fig. 5). So, the boundaries conditions are

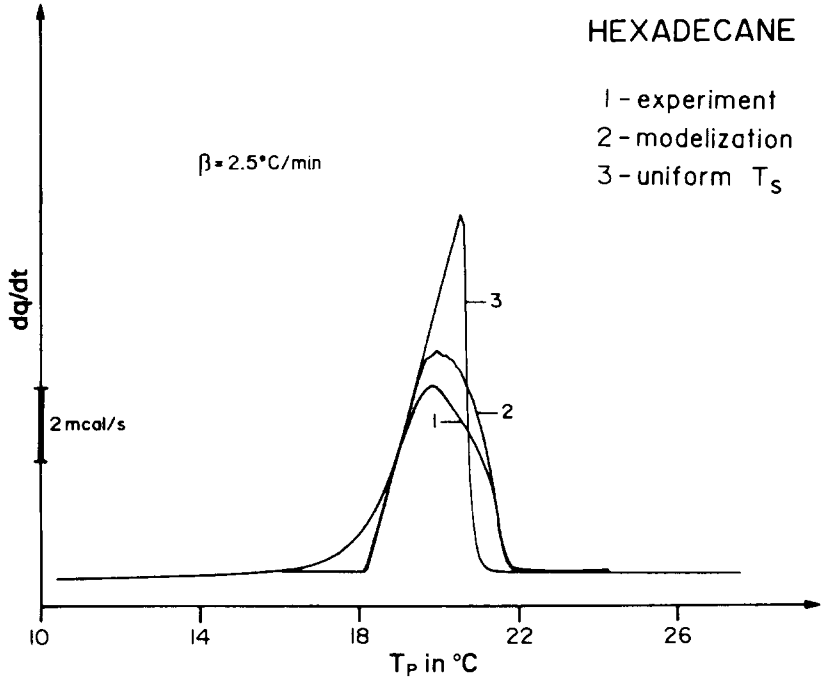

Fig. 6. Experimental thermogram for the melting of an emulsion of hexadecane compared to the calculated thermogram obtained with our model and to the calculated thermogram obtained with the classical assumption, at $\beta = 2.5°\mathrm{C\,min}^{-1}$.

$$\left(\frac{\partial T}{\partial r}\right)_{r=0} = 0 \tag{9}$$

$$-k\left(\frac{\partial T}{\partial r}\right)_{\substack{r=R_0\\z=0}} = h^{\mathrm{ext}}(T - T_{\mathrm{P}}) \tag{10}$$

$$-k\left(\frac{\partial T}{\partial z}\right)_{z=0} = h^{\mathrm{ext}}(T - T_{\mathrm{P}}) \tag{11}$$

$$-k\left(\frac{\partial T}{\partial z}\right)_{z=Z} = h'^{\mathrm{ext}}(T - T_{\mathrm{P}}) \tag{12}$$

where $T_{\mathrm{P}}$, the temperature of the plates, is programmed to be a linear function

$$T_{\mathrm{P}} = \beta t + T_0 \quad (\beta > 0) \tag{13}$$

At $t = 0$ the initial conditions are

$$T(r, z, 0) = T_{\mathrm{g}}(r, z, 0) = T_{\mathrm{P}}(0) = T_0 \quad \text{and } X(r, z, 0) = 0 \tag{14}$$

Because the thermal conductivity of air is very much smaller than that of the metal of the cell, we consider that all the energy is transmitted to the plate by the lower boundary of the cell. So, $\mathrm{d}q/\mathrm{d}t$ is the sum of the thermal fluxes through the walls of the metallic cell

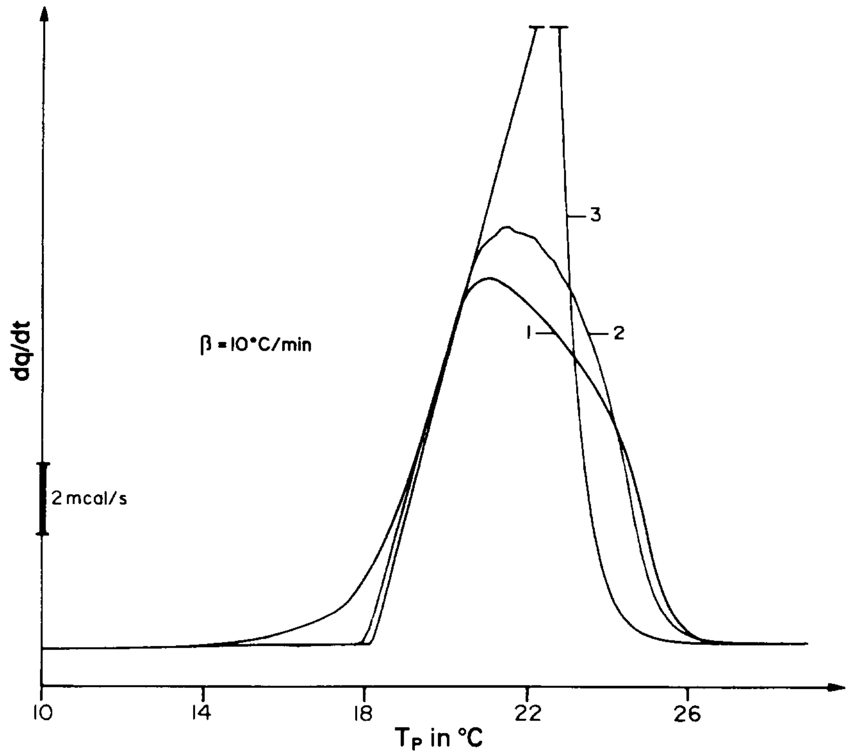

Fig. 7. Same curves as in Fig. 6, but at 10°C min$^{-1}$.

$$\frac{dq}{dt} = -\sum_i h_i(T - T_P)\Delta S_i \qquad (15)$$

where $h_i = h^{\text{ext}}$ or $h'^{\text{ext}}$.

To solve the equations and to determine $T(r, z, t)$, $T_g(r, z, t)$ or $X(r, z, t)$, we used an explicit finite differences method.

## RESULTS

The present model depends on an adjustable parameter in addition to $h^{\text{ext}}$ or $h'^{\text{ext}}$, also determined for the model concerning crystallization [1], which is the exchange coefficient $h$ for the interface between the droplet and the emulsifying medium. It is possible to adjust $h$ to have the best fit between the calculated and experimental thermograms, particularly for the slope of the straight part of the peak, its height or its width. Its value is about 0.05 W m$^{-2}$ K$^{-1}$. This low value can be explained by the relatively large thickness of the surfactant layer surrounding the droplet.

Figure 6 shows an experimental thermogram for the melting of an emulsion of hexadecane ($T_F$ = 18.0°C), at 2.5°C min$^{-1}$, compared with the calculated thermogram obtained with our model, and with the calculated thermogram obtained with the classical assumption. We can see that the

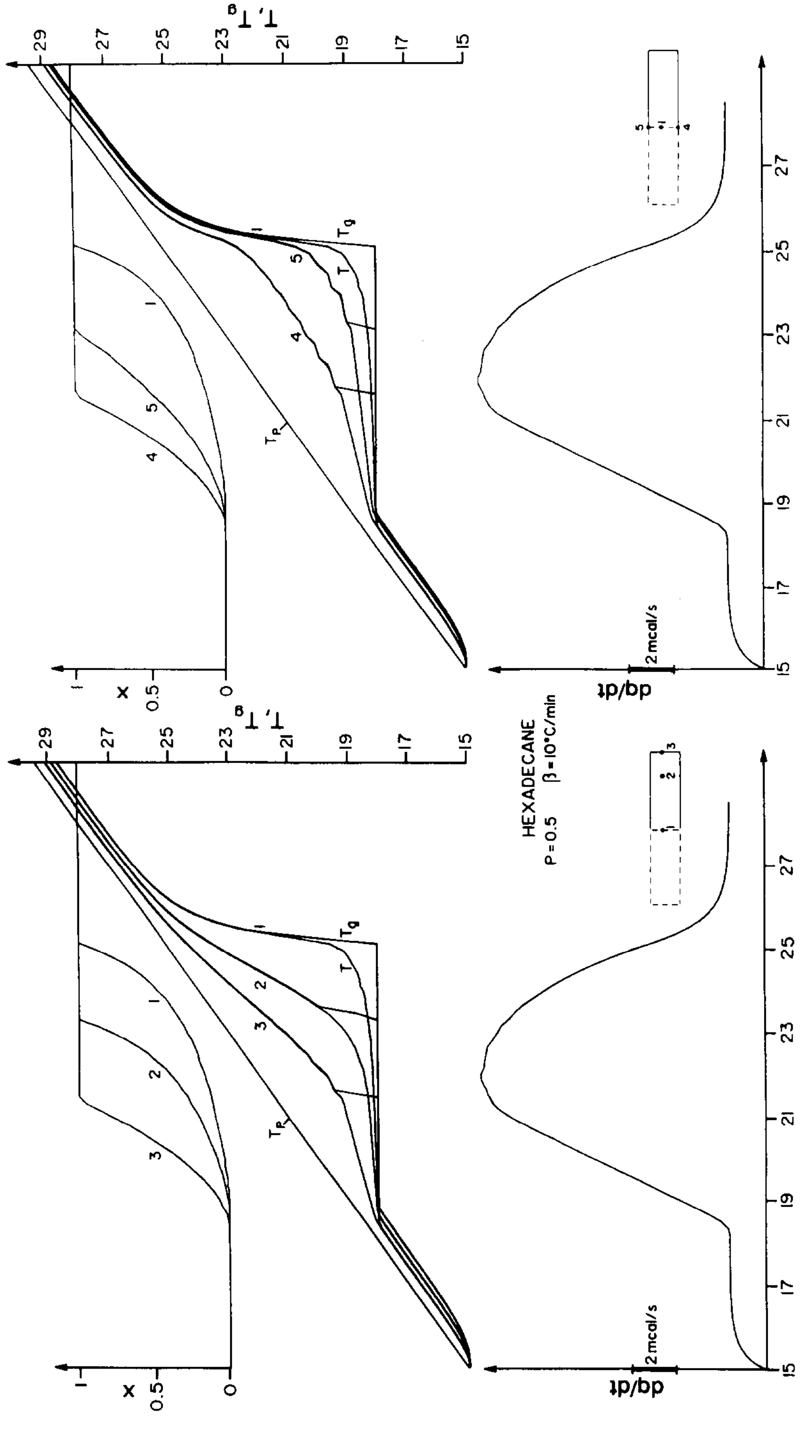

Fig. 8. Calculated values of $T(r, z, t)$, $T_g(r, z, t)$ and $X(r, z, t)$ for different points in a median plane or on the axis, in comparison with the thermogram.

latter thermogram does not fit at all with the experimental peak, in either height or width. Therefore, we definitively discard the interpretation of the melting peak by the classical assumption.

The fit between the experimental and the calculated curves is relatively good: the rounded form of the top of the peak is reproduced and its width is the same. The height is slightly different, which can be explained by the impurities in the hexadecane which also cause the curved shape at the start of the peak, as already noticed. Figure 7 shows the same comparison for another heating rate ($\beta = 10°\mathrm{C\,min^{-1}}$) which confirms the good fit.

Figure 8 presents the temperatures $T$ and $T_g$ at different points of the cell, and the corresponding melted fraction $X$ plotted against $T_P$ i.e. versus time, from the linear relationship (13). This figure also includes the corresponding calculated thermogram. Important temperature differences can be observed as a function of the radius or the height of the cell. These differences can reach 7°C ($\beta = 10°\mathrm{C\,min^{-1}}$) at certain points. There is a small difference between the temperature of the emulsifying medium $T$, and the inner temperature of the droplet $T_g$. It reaches a maximum of about 1.5°C when the last part of the solid melts. Melting begins as soon as $T_g = T_F$ but it is very fast near the metallic boundaries and is slower in the central region. In the central region, the melting finishes after the instant of the peak maximum, in opposition to the classical assumption which predicts that the end of the melting is exactly at the top of the peak.

## CONCLUSIONS

The model we have developed for the melting of crystallized droplets of an emulsion, when it is applied to differential scanning calorimetry, explains the shape of the thermograms, whereas the classical hypothesis which assumes the uniformity of the temperature in the cell, most certainly does not.

Despite the small dimensions of the cell, we have found important temperature gradients, responsible for the shape of the peaks. These gradients become more and more important as the heating rate increases. The model also predicts the kinetics of the melting of the droplets which depends on their location.

## REFERENCES

1 J.P. Dumas, Y. Zeraouli and M. Strub, Heat transfer inside emulsions. Determination of the DSC thermograms. Part 1. Crystallizations of the undercooled droplets, Thermochim. Acta, 236 (1994) 227–237.

2 A.P. Gray, A simple generalized theory for the analysis of dynamic thermal measurements, Analytical Calorimetry, Vol. 1, Plenum Press, New York, 1968, p. 209.

3 J.P. Dumas, The analysis of theoretical melting curves in differential scanning calorimetry, J. Phys. D: Appl. Phys., 11 (1978) 1–5.

4 Y. Haget, R. Courchinoux, J.R. Housty, N.B. Chanh, M.A. Cuevas-Diarte, E. Tauler, T. Calvet and E. Estop, Une méthode simple pour aller du signal aux phénomènes dans le cas de l'établissement des diagrammes binaires par analyse thermique, Congrès Calorimétrie et Analyse Thermique, Bordeaux, 25–27 May 1987, Vol. XIII, p. 255.
5 Y. Zeraouli, Etude thermique des transformations des émulsions concentrées. Application à la calorimétrie à balayage, Thesis, 1991, University of Pau, France.